HIGH ENERGY π^--p, K^--p AND $\bar{p}$-p ELASTIC SCATTERING[x]

R. Rubinstein, A. Ashmore,[*] C.J.S. Damerell[†] and W.R. Frisken[‡]
Brookhaven National Laboratory, Upton, New York.

J. Orear, D.P. Owen, F.C. Peterson, A.L. Read,[**] D.G. Ryan[††] and D.H. White
Cornell University, Ithaca, New York.

We report here results from a recent Brookhaven A.G.S. experiment on the study of high energy elastic scattering of π, K and $\bar{p}$ from protons; some data from $\pi^{\pm}$-p scattering near 180° c.m. has already been reported.[1)] In the present work, elastic scattering of $\pi^{\pm}$ from protons between 5.9 and 14 GeV/c has been measured for centre-of-mass angles 135°-165°; measurements of elastic scattering of π^-, K^- and $\bar{p}$ from protons at 5.9 GeV/c for centre-of-mass angles 20°-110° have been made and also over a more limited angular range at 7.9 and 9.8 GeV/c.

The experimental arrangement for the 135°-165° range is shown in Figure 1. A beam defined by scintillation counters was incident on a 2-ft.-long liquid hydrogen target. Scattered and recoil particles were momentum analyzed by magnets M_1 and M_2 and detected by a number of scintillation counter telescopes shown as π_1, π_2, π_3, etc. There were up to 10 such telescopes for the pion and up to 5 for the proton. C was a threshold gas Cerenkov counter which vetoed forward-scattered pions. A coincidence between a beam particle, a pion telescope and a proton telescope caused the optical spark chambers SC_1-SC_6 to be pulsed. The arrangement for 20-110° cms is shown in Figure 2. It is similar in principle to that given

above, but both particles are now momentum analyzed by the same magnet. Not shown in the figure are a threshold and two differential gas Cerenkov counters in the incident beam to identify the type of incoming particle. Beam intensities were $\sim 5 \times 10^5$ particles per pulse and trigger rates in the range 1 per 3 pulses to 1 per 100 pulses.

In the analysis of the photographs, the pion track was assumed to originate from an elastic event; its trajectory was extrapolated back through the magnet to the target and required to pass through a fiducial volume. For tracks satisfying this criterion, the corresponding elastic scattering proton trajectory was calculated and the difference between this and the track observed in the proton spark chamber calculated. In this way it was possible to separate elastic from inelastic events. Elastic events were between 1% and 70% of the total number, depending on angle and energy.

Corrections were applied to the data for empty target rate, for muon and electron contamination of the pion beam, for decay of the scattered pion, and for absorption of particles in scintillators, target, and other material. Solid angle acceptance was determined by a Monte Carlo calculation. All results presented are given with statistical errors only; additional systematic errors of $\pm 15\%$ are not included.

Results for π^- scattering in the backward region are shown in Figure 3. Previously reported data[1)] near 180° is also shown. The discrepancy between the two sets of data in the overlap region is still being studied, and preliminary indications are that it will substantially disappear. We see the pronounced backward peak, which can be fitted by the expression

$\frac{d\sigma}{du} \sim e^{-4|u|}$; this is to be compared with the sharper forward diffraction peak $\frac{d\sigma}{dt} \sim e^{-9|t|}$. Statistics are not accurate enough to see if there is any energy dependence of the exponent.

Results for π^+ scattering in the backward region are shown in Figure 4. We see at all energies the sharp backward peak, dropping to a valley at $u \approx -0.2$ $(GeV/c)^2$, with a second maximum at larger $|u|$ values. Near 180°, fitted expressions of the form $\frac{d\sigma}{du} \sim e^{-A|u|}$ give values of A in the range 15-20 $(GeV/c)^{-2}$, so the slopes are about twice as large as in the forward diffraction region. There is an increase in the value of A with increasing incident momentum.

When comparing the π^- and π^+ results, we note that in the region of the π^+ valley at $u \approx -0.2$ $(GeV/c)^2$, the π^+ cross section is $\sim 1/9$ that for π^-, indicating little $I=\frac{1}{2}$ exchange at this point.

The π^+ and π^- data presented above have been fitted by Barger,[2] using a Regge pole analysis. The parameters derived for the N_α, N_γ and Δ_δ trajectories are in good agreement with those obtained from linear Chew-Frautschi plots.

The results obtained for 5.9 GeV/c π^- in the forward direction are shown in Figure 5. Some structure in the differential cross section is observed at $-t \approx 1.0$ $(GeV/c)^2$, which is less pronounced than a corresponding effect at lower energies. In addition a prominent dip is seen at $-t \approx 3.0$ $(GeV/c)^2$. Very similar behaviour is evident in the 7.9 GeV/c data shown in Figure 6; also shown in this figure is data obtained in an earlier experiment at this energy but at smaller angles[3] and the freehand curve of 5.9 GeV/c data from Figure 5. We see that the differential cross

section at large momentum transfers falls by a factor of 2-3 between these two momenta. Figure 7 shows some data at larger angles at 9.8 GeV/c, compared with data from Figure 6, showing again a factor of 2-3 decrease in differential cross section between 7.9 and 9.8 GeV/c. We also shown in the $|t|$ range 15 to 18 $(GeV/c)^2$ some of the backward scattering results from Figure 3.

In Figure 8, we show the 5.9 GeV/c $\bar{p}$-p data. Here we see a prominent dip at $-t \approx 0.5$ $(GeV/c)^2$, which has been seen previously at lower energies,[4] and evidence for another dip at $-t \approx 1.8 (GeV/c)^2$.

K^--p results at 5.9 GeV/c are shown in Figure 9 and give evidence for some structure at $-t \approx 0.9$ $(GeV/c)^2$ as in the π^--p case. The statistical accuracy is not sufficient to see if there is any structure at larger angles.

In all the cross sections measured, data at our lowest $|t|$ values agree with other measurements made closer to the forward direction.[5]

The freehand curves through the data of Figures 5, 8 and 9 are shown superimposed in Figure 10. It can be seen that the cross sections have roughly the same magnitude while all falling by three decades. Proton-proton cross sections[6] at this momentum are not shown but are over an order of magnitude higher at large momentum transfers. However, if an interpolation of proton-proton results at ~ 9 GeV/c is used, overall agreement with the π^--p results is reasonable except in the region of the dip at $-t \sim 3$ $(GeV/c)^2$. This comparison momentum can be derived from either a quark model prediction that the incident momentum in proton-proton collisions should be 3/2 that in the pion-proton case, or by comparing the two reactions at the same Q value.

While no detailed analysis of these results has yet been made, it is interesting to note that a simple black disc diffraction pattern for a radius of 1.1 fermi would give minima at $-t \approx 0.5$ and 1.9 $(\mathrm{GeV}/c)^2$, as found for $\bar{p}$-p scattering, and a radius of 0.85 fermi would give minima at $-t \approx 0.9$ and 3.0 $(\mathrm{GeV}/c)^2$, which is in reasonable agreement with the π^--p results.

REFERENCES

x Work supported by the U. S. Atomic Energy Commission and research grant from the National Science Foundation.

* Permanent address: Queen Mary College, London, England.

† Rutherford High Energy Laboratory Fellow.

‡ Present address: Department of Physics, Case Western Reserve University, Cleveland, Ohio.

** Present address: National Accelerator Laboratory, Oak Brook, Illinois.

†† Present address: Department of Physics, McGill University, Montreal, Quebec, Canada.

1. A. Ashmore, C.J.S. Damerell, W.R. Frisken, R. Rubinstein, J. Orear, D.P. Owen, F.C. Peterson, A.L. Read, D.G. Ryan and D.H. White. Phys. Rev. Letters 19, 460 (1967).

2. V. Barger. Reported by M. Derrick at this Conference.

3. J. Orear, R. Rubinstein, D.B. Scarl, D.H. White, A.D. Krisch, W.R. Frisken, A.L. Read and H. Ruderman. Phys. Rev. 152, 1162 (1966).

4. W.M. Katz, B. Forman and T. Ferbel. Phys. Rev. Letters 19, 265 (1967).

5. K.J. Foley, S.J. Lindenbaum, W.A. Love, S. Ozaki, J.J. Russell and L.C.L. Yuan. Phys. Rev. Letters 10, 376 (1963); 11, 425 (1963); 11, 503 (1963).

6. C.M. Ankenbrandt, A.R. Clark, B. Cork, T. Elioff, L.T. Kerth and W.A. Wenzel. U.C.R.L. 17763.

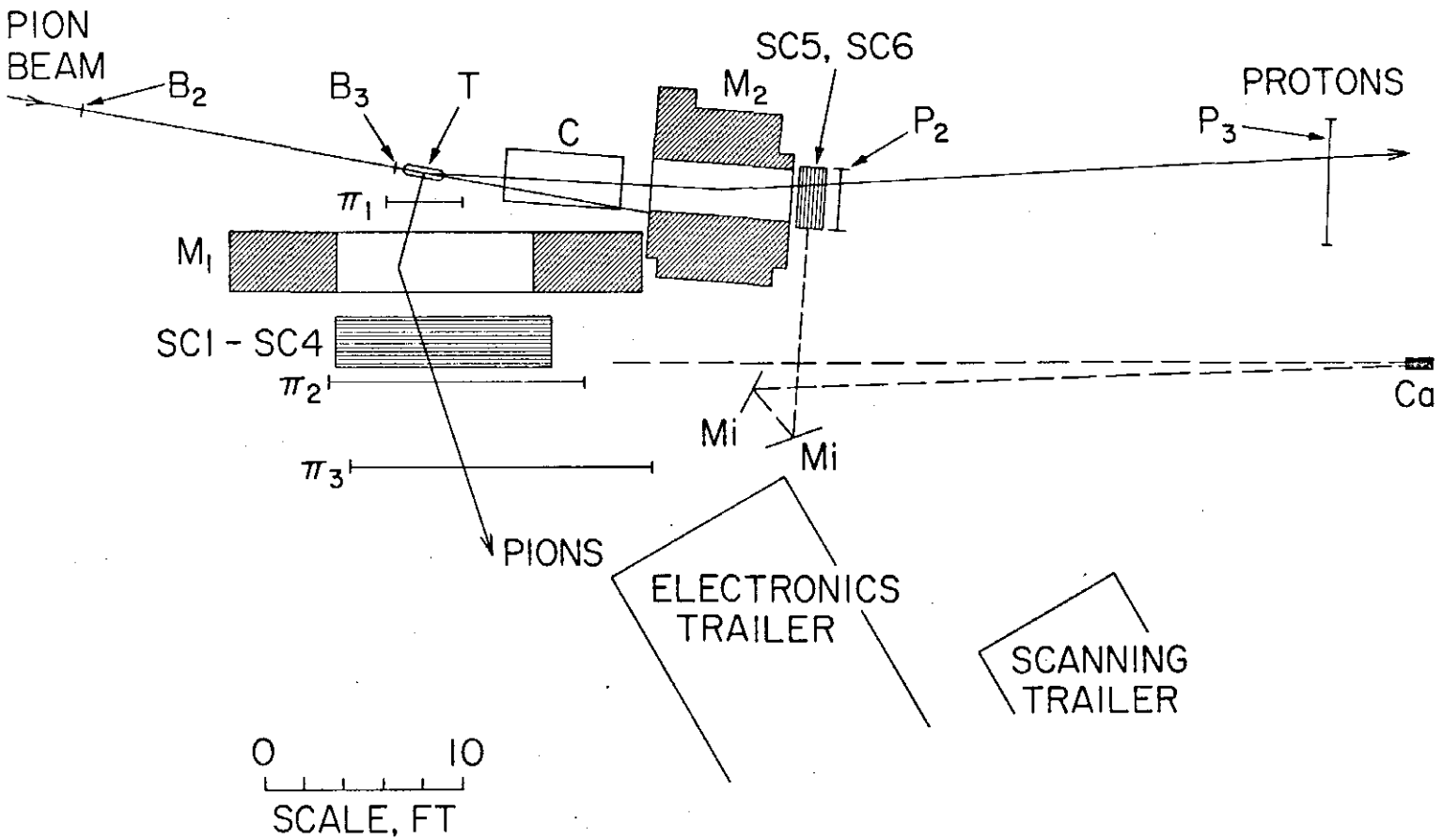
PION
BEAM
B2
B3
T
C
M2
SC5, SC6
P2
PROTONS
P3
π1
M1
SC1 - SC4
π2
π3
Mi
Mi
Ca
PIONS
ELECTRONICS
TRAILER
SCANNING
TRAILER
0
10
SCALE, FT

FIGURE 1

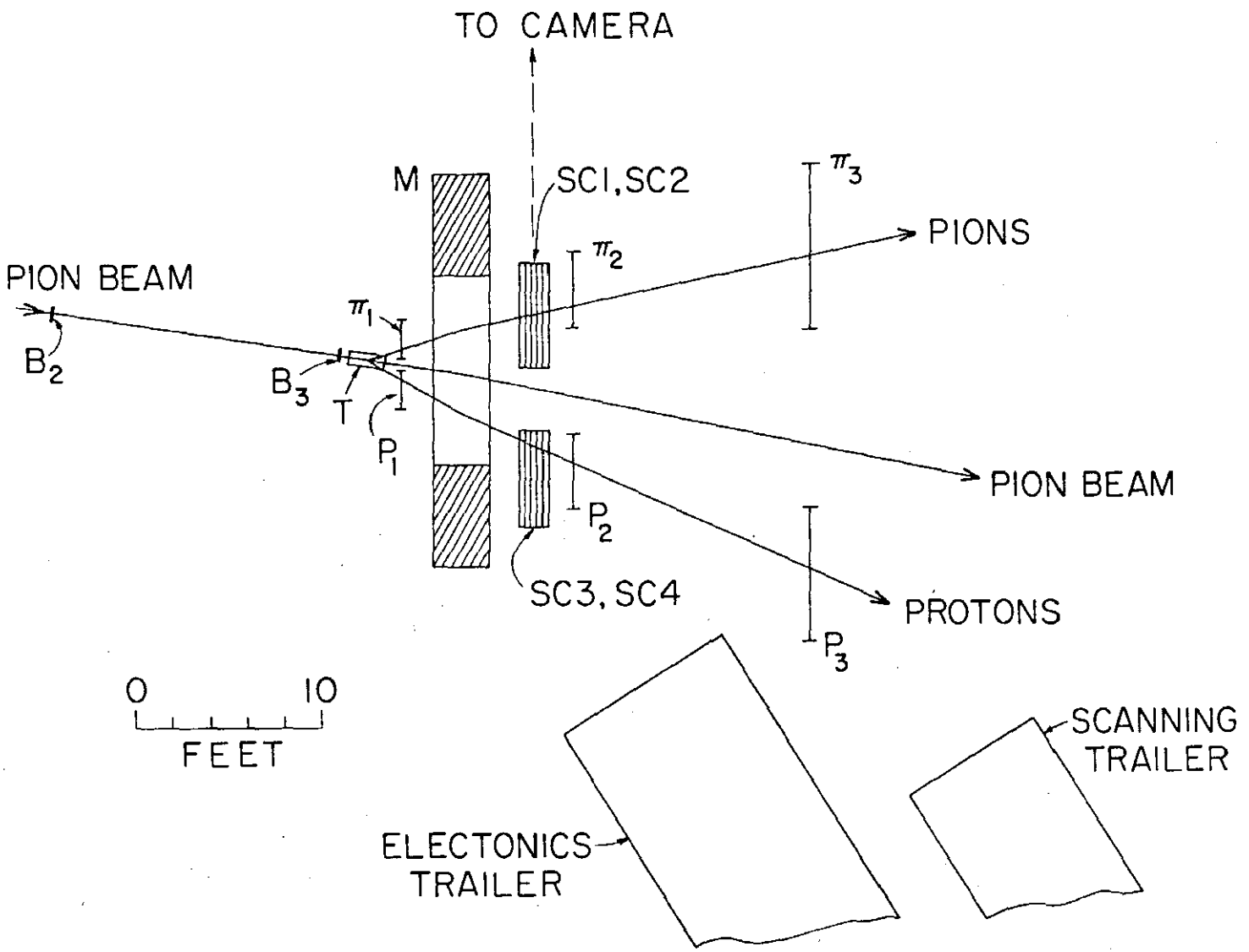
TO CAMERA
M
SC1, SC2
π_3
PIONS
π_2
PION BEAM
π_1
B_2
B_3
T
P_1
PION BEAM
P_2
SC3, SC4
PROTONS
P_3
0
10
FEET
SCANNING TRAILER
ELECTONICS TRAILER

FIGURE 2

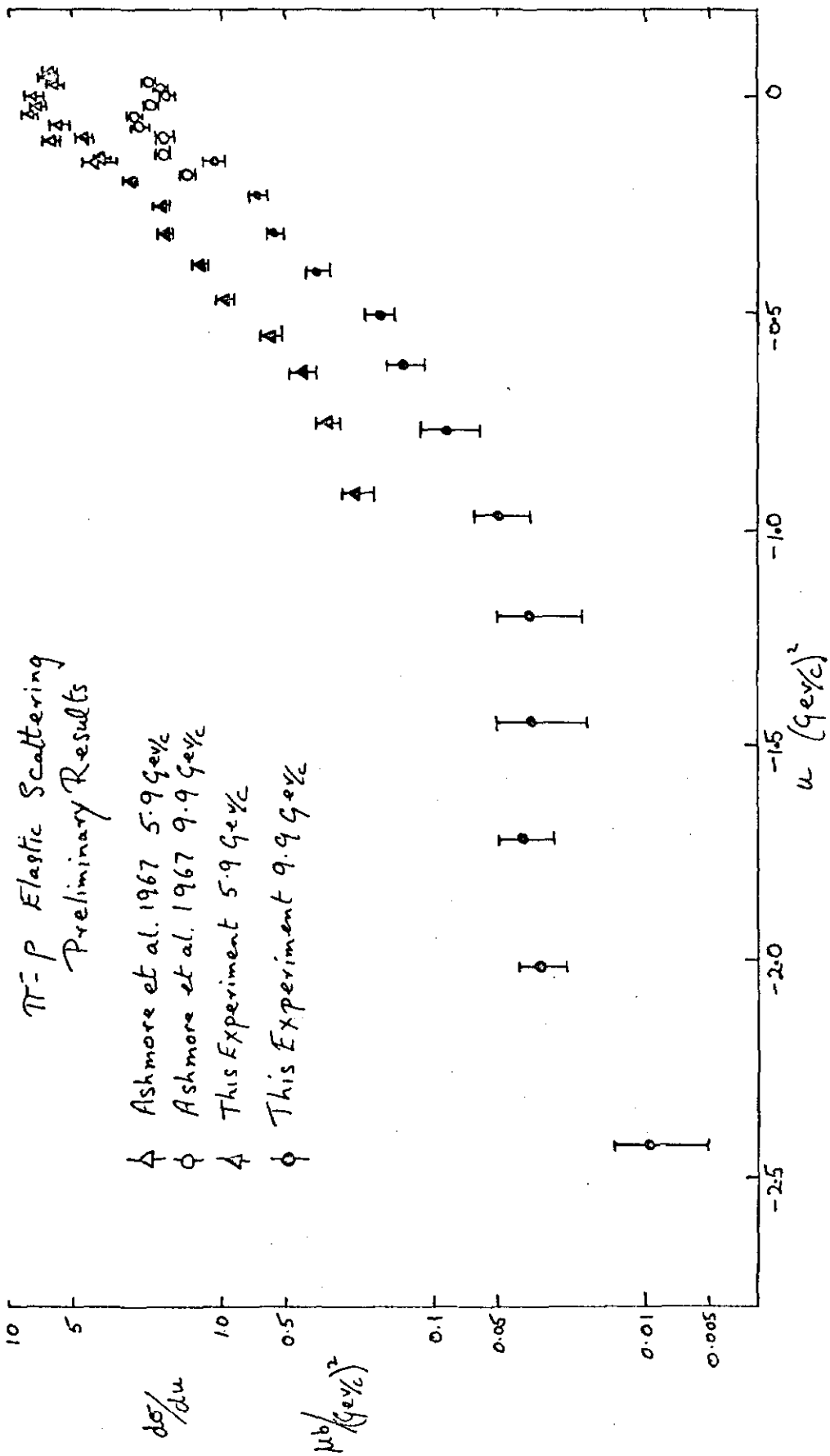
π⁻p Elastic Scattering
Preliminary Results
Ashmore et al. 1967 5.9 GeV/c
Ashmore et al. 1967 9.9 GeV/c
This Experiment 5.9 GeV/c
This Experiment 9.9 GeV/c
dσ/du
μb/(GeV/c)²
10
5
1.0
0.5
0.1
0.05
0.01
0.005
-2.5
-2.0
-1.5
-1.0
-0.5
0
u (GeV/c)²

FIGURE 3

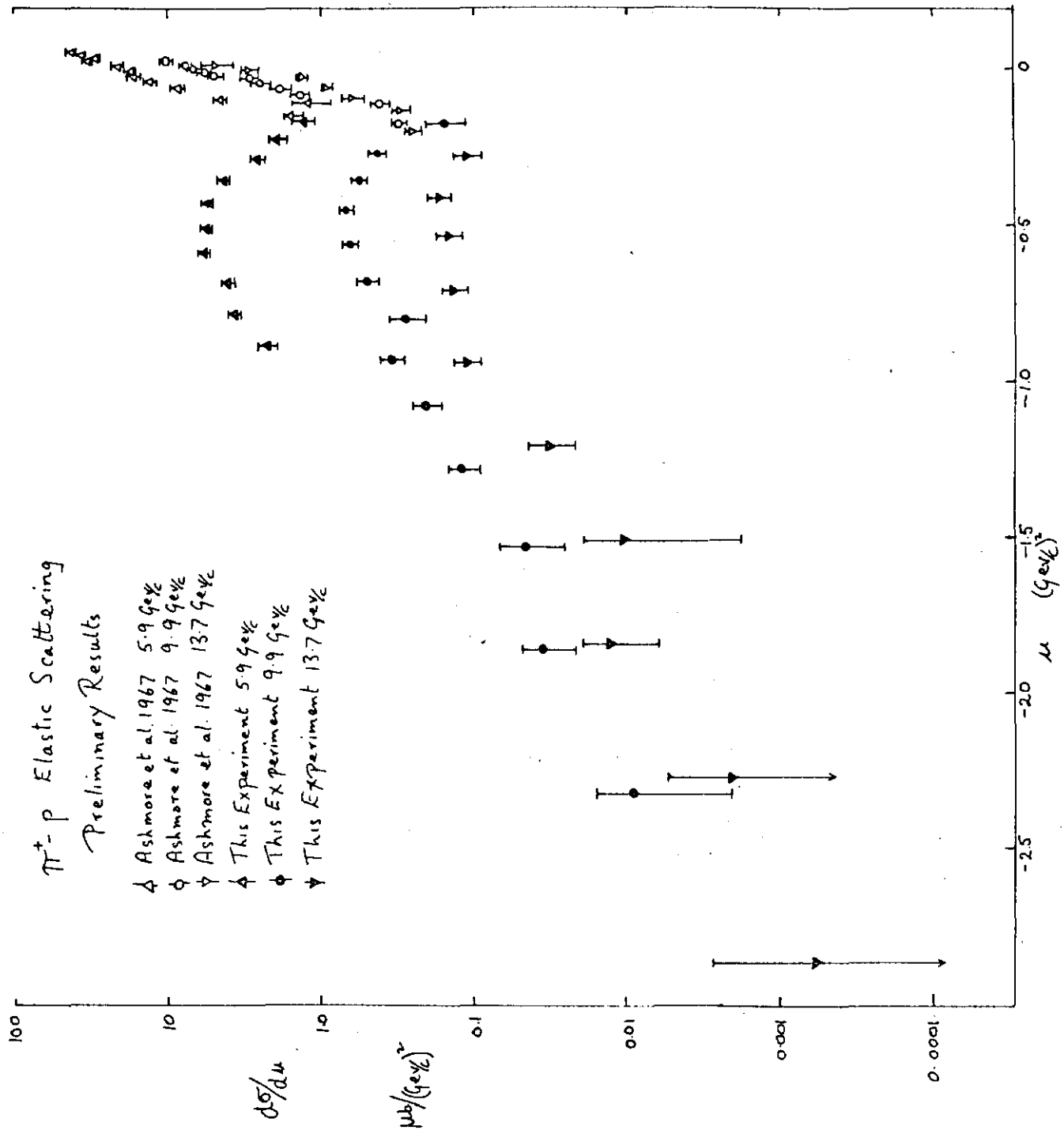
π⁺-p Elastic Scattering
Preliminary Results
Ashmore et al. 1967 5.9 GeV/c
Ashmore et al. 1967 9.9 GeV/c
Ashmore et al. 1967 13.7 GeV/c
This Experiment 5.9 GeV/c
This Experiment 9.9 GeV/c
This Experiment 13.7 GeV/c
dσ/dμ
μb/(GeV/c)²
100
10
1.0
0.1
0.01
0.001
0.0001
-2.5
-2.0
-1.5
-1.0
-0.5
0
μ (GeV/c)²

FIGURE 4

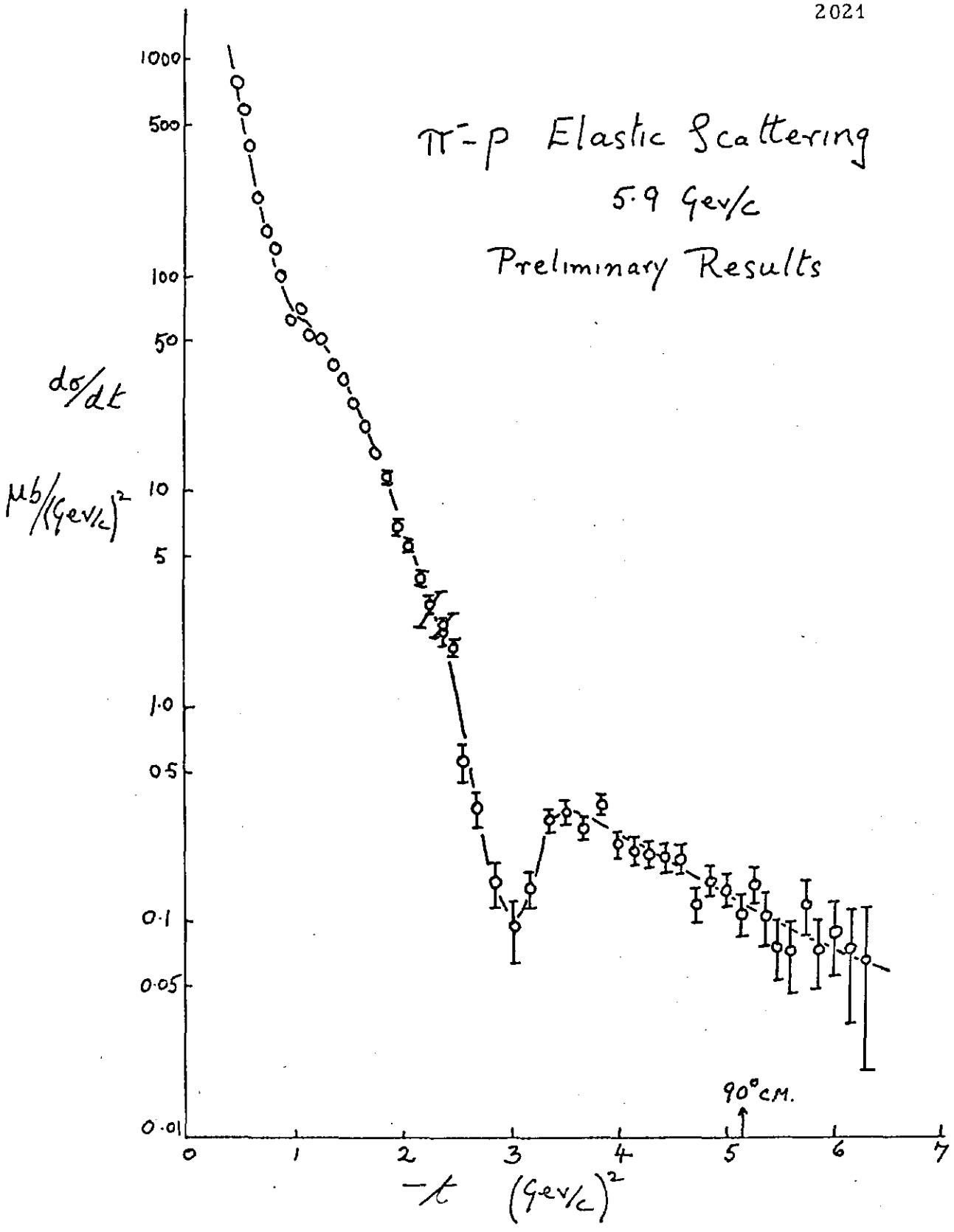
π⁻-p Elastic Scattering
5.9 Gev/c
Preliminary Results
dσ/dt
μb/(Gev/c)²
1000
500
100
50
10
5
1.0
0.5
0.1
0.05
0.01
90° CM.
0
1
2
3
4
5
6
7
−t (Gev/c)²

FIGURE 5

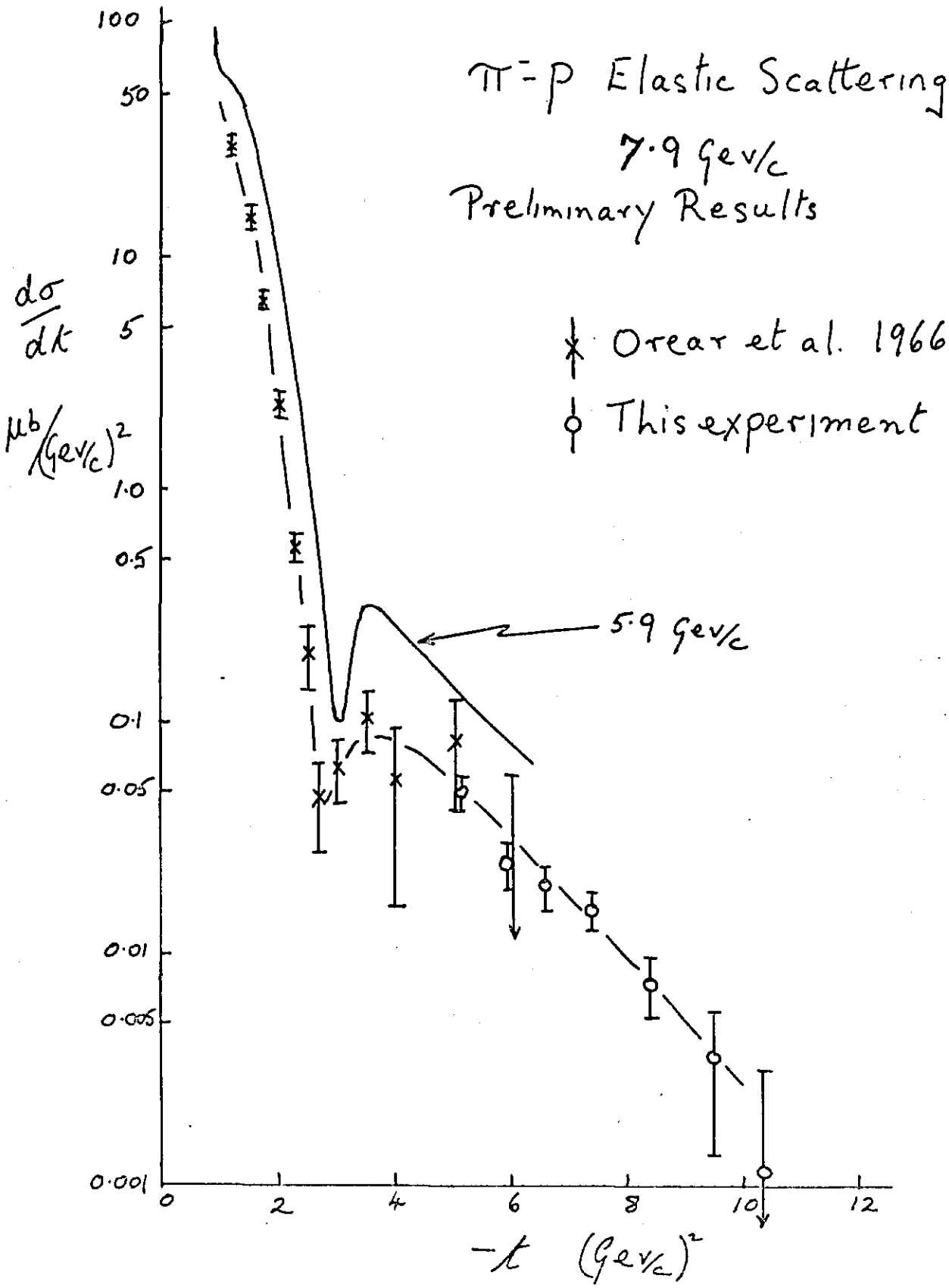
π⁻p Elastic Scattering
7.9 Gev/c
Preliminary Results
Orear et al. 1966
This experiment
5.9 Gev/c
dσ/dt
μb/(Gev/c)²
100
50
10
5
1.0
0.5
0.1
0.05
0.01
0.005
0.001
0
2
4
6
8
10
12
−t (Gev/c)²

FIGURE 6

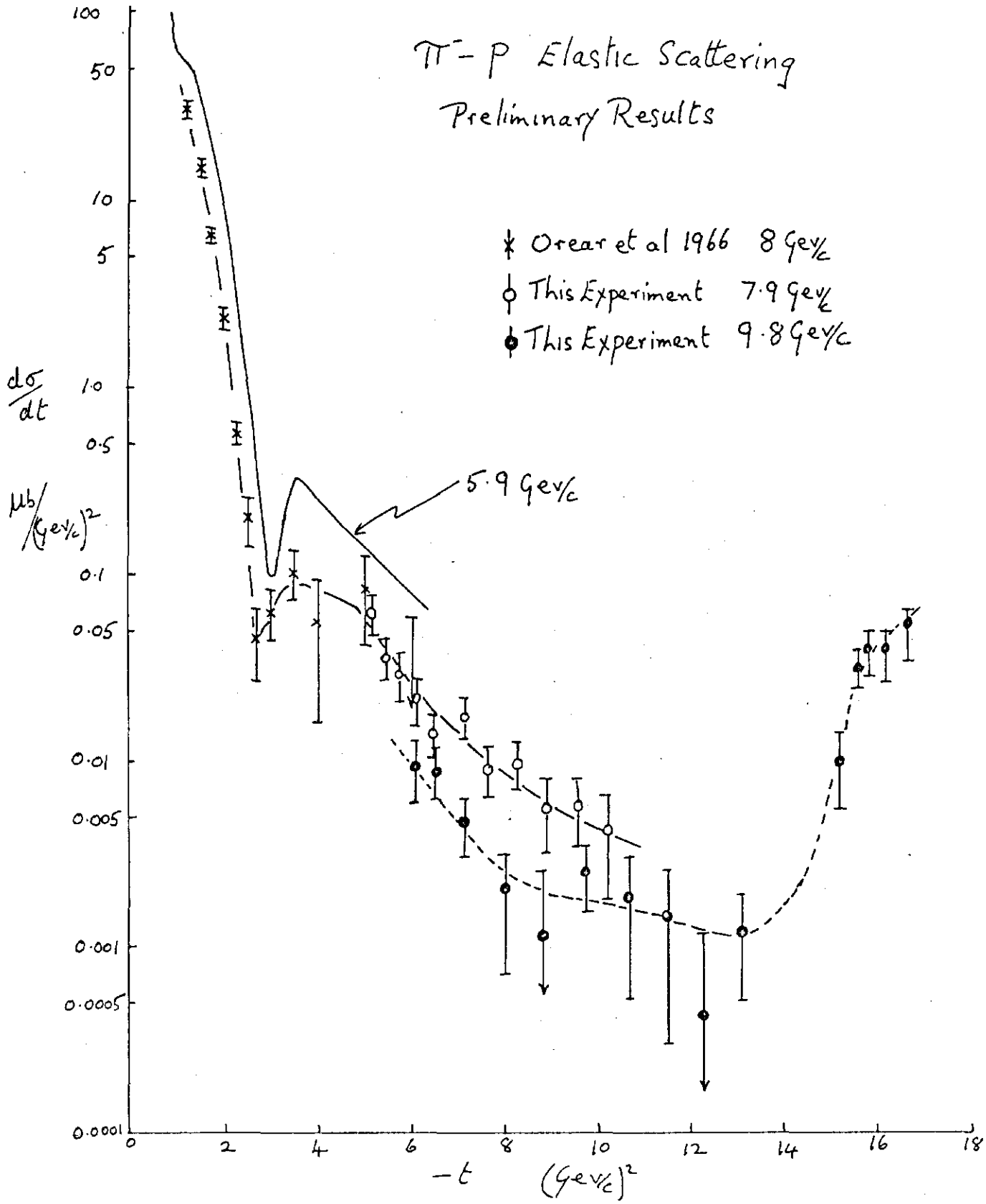
π⁻ - p Elastic Scattering
Preliminary Results
Orear et al 1966 8 Gev/c
This Experiment 7.9 Gev/c
This Experiment 9.8 Gev/c
5.9 Gev/c
dσ/dt
μb/(Gev/c)²
100
50
10
5
1.0
0.5
0.1
0.05
0.01
0.005
0.001
0.0005
0.0001
0
2
4
6
8
10
12
14
16
18
−t (Gev/c)²

FIGURE 7

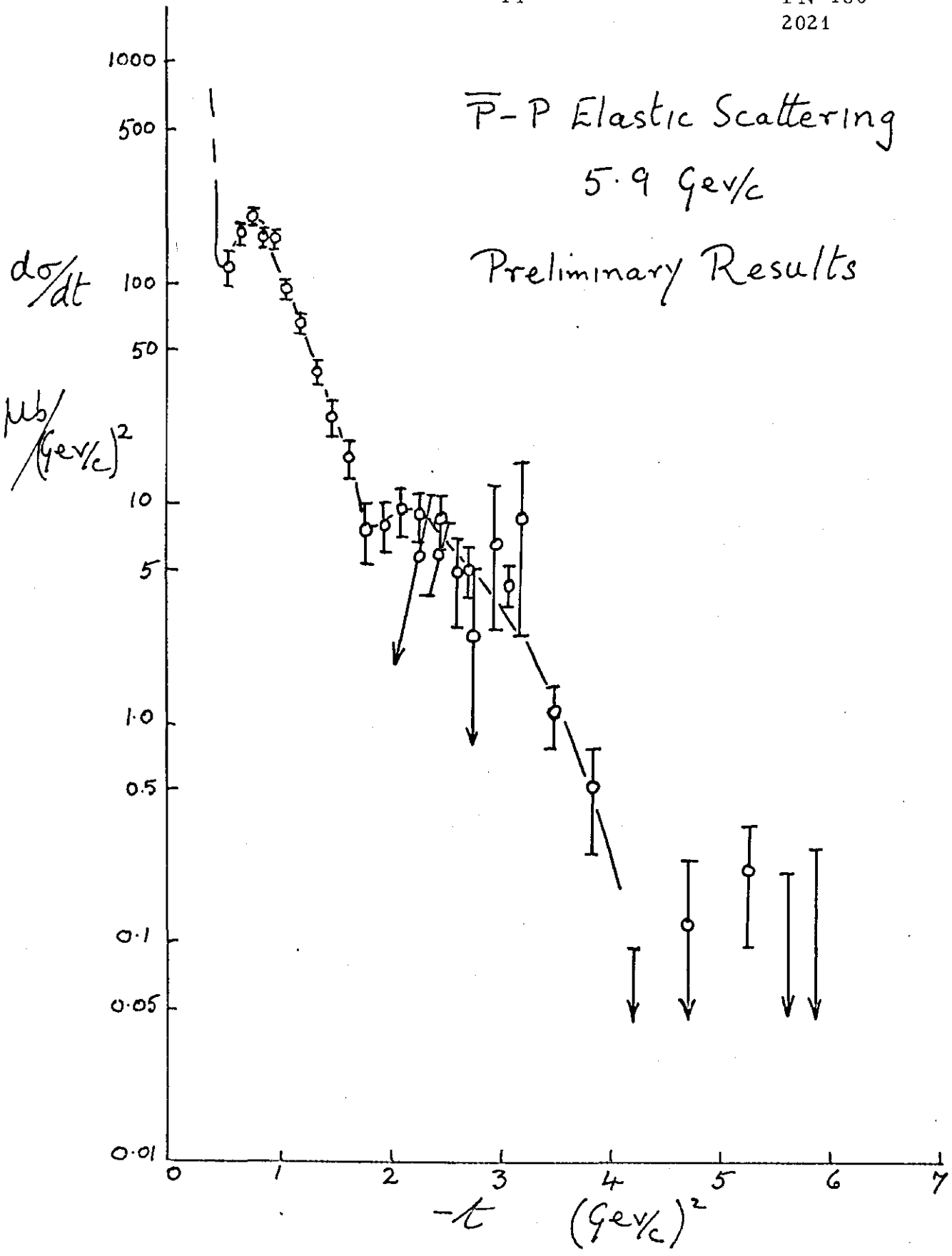
$\bar{P}$-P Elastic Scattering
5.9 Gev/c
Preliminary Results
dσ/dt
μb/(Gev/c)²
1000
500
100
50
10
5
1.0
0.5
0.1
0.05
0.01
0
1
2
3
4
5
6
7
-t (Gev/c)²

FIGURE 8

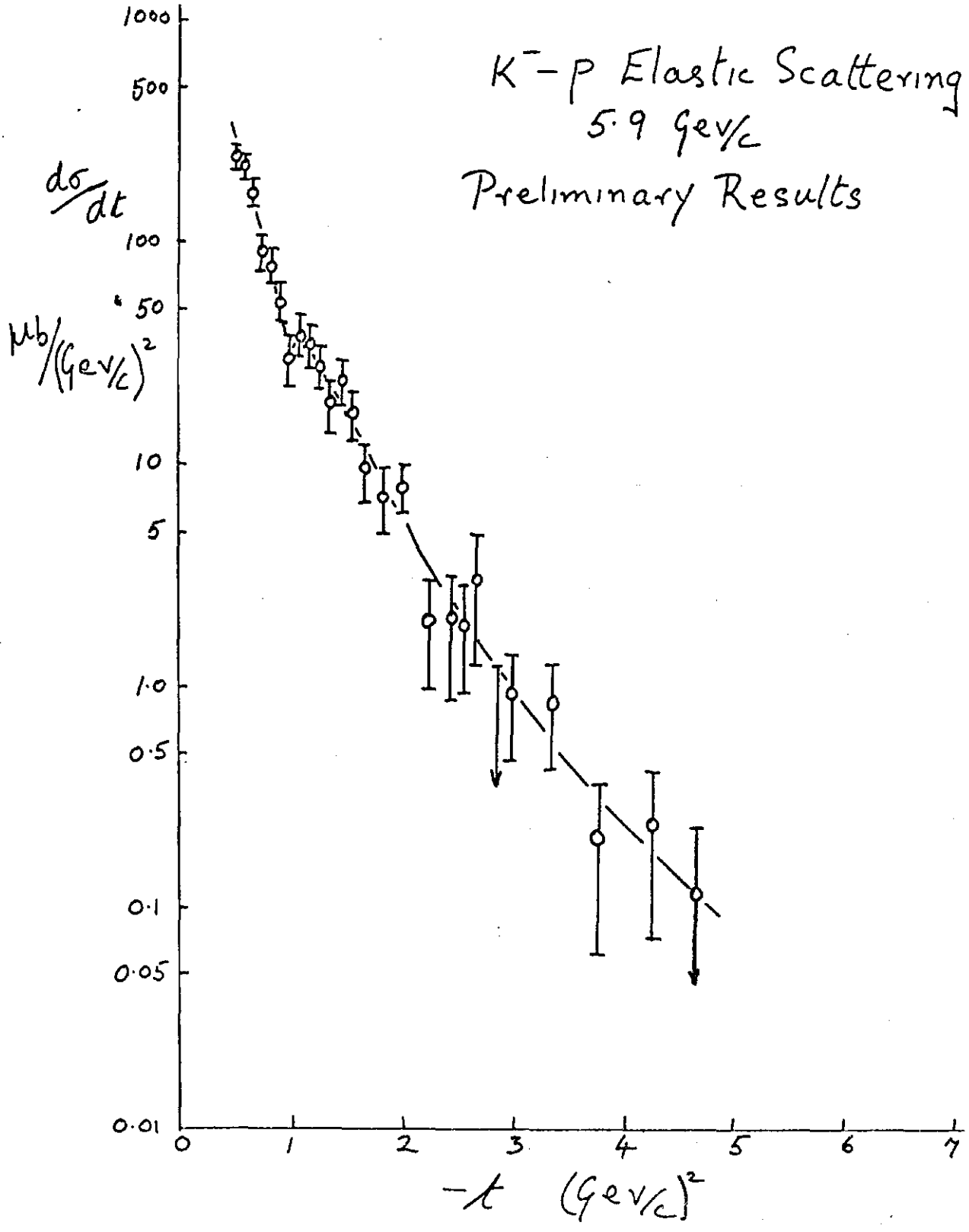
K⁻-p Elastic Scattering
5.9 Gev/c
Preliminary Results
dσ/dt
μb/(Gev/c)²
1000
500
100
50
10
5
1.0
0.5
0.1
0.05
0.01
0
1
2
3
4
5
6
7
-t (Gev/c)²

FIGURE 9

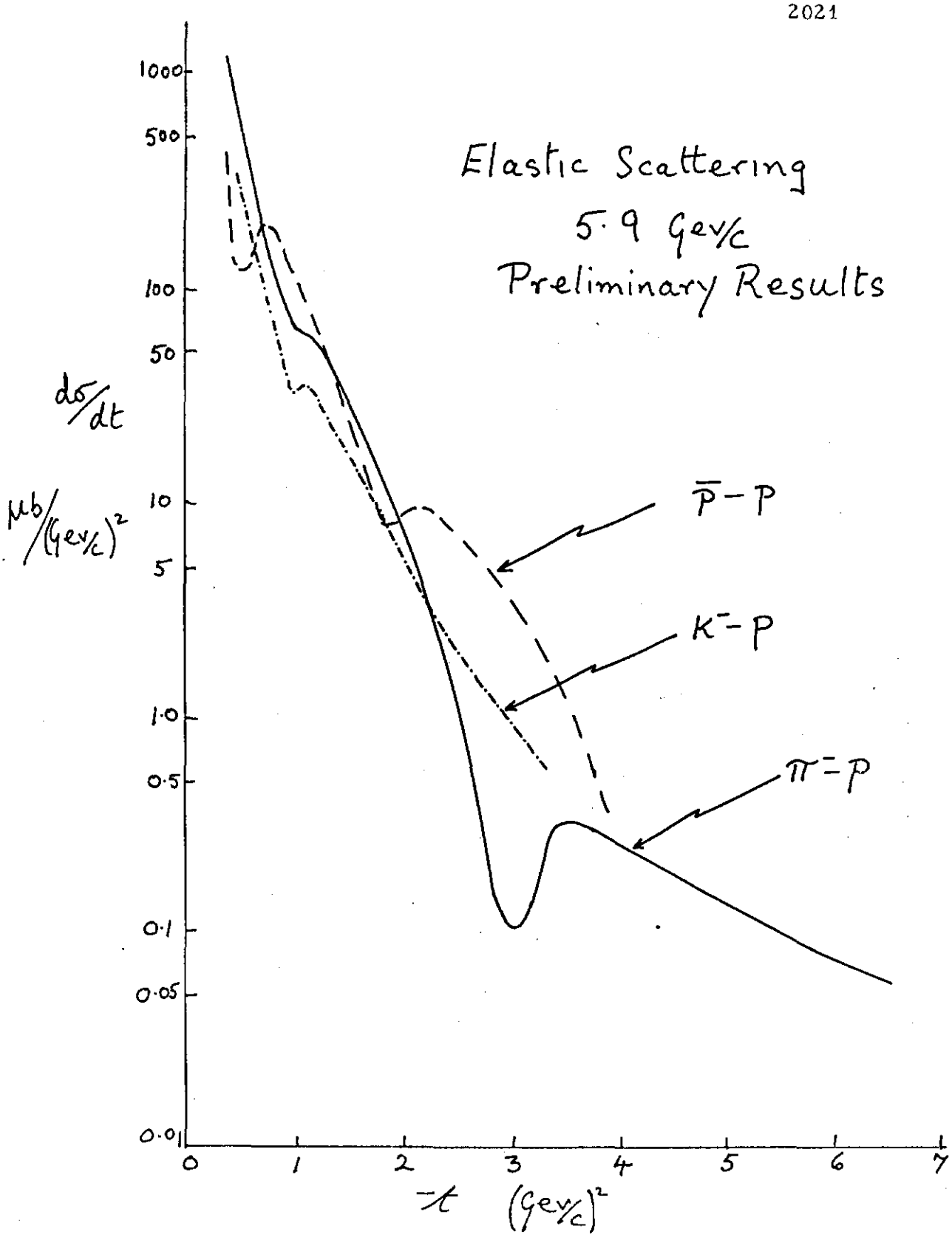
Elastic Scattering
5.9 Gev/c
Preliminary Results
dσ/dt
μb/(Gev/c)²
1000
500
100
50
10
5
1.0
0.5
0.1
0.05
0.01
0
1
2
3
4
5
6
7
-t (Gev/c)²
p̄-p
K⁻-p
π⁻-p

FIGURE 10